Published in final edited form as:
J Immunol. 2011 January 15; 186(2): 1044–1059. doi:10.4049/jimmunol.1003052.

Blocking of α4β7 Gut-Homing Integrin during Acute Infection Leads to Decreased Plasma and Gastrointestinal Tissue Viral Loads in Simian Immunodeficiency Virus-Infected Rhesus Macaques

Aftab A. Ansari[*], **Keith A. Reimann**[†], **Ann E. Mayne**[*], **Yoshiaki Takahashi**[*], **Susan T. Stephenson**[*], **Rijian Wang**[†], **Xinyue Wang**[†], **Jichu Li**[†], **Andrew A. Price**[†], **Dawn M. Little**[*], **Mohammad Zaidi**[*], **Robert Lyles**[‡], and **Francois Villinger**[*,§]

[*]Department of Pathology and Laboratory Medicine, Emory University School of Medicine, Atlanta, GA 30322

[†]Division of Viral Pathogenesis, Beth Israel Deaconess Medical Center, Boston, MA 02215

[‡]Department of Biostatistics, Rollins School of Public Health, Emory University, Atlanta, GA 30322

[§]Division of Pathology, Yerkes National Primate Research Center, Emory University, Atlanta, GA 30329

Abstract

Intravenous administration of a novel recombinant rhesus mAb against the α4β7 gut-homing integrin (mAb) into rhesus macaques just prior to and during acute SIV infection resulted in significant decrease in plasma and gastrointestinal (GI) tissue viral load and a marked reduction in GI tissue proviral DNA load as compared with control SIV-infected rhesus macaques. This mAb administration was associated with increases in peripheral blood naive and central memory $CD4^+$ T cells and maintenance of a high frequency of $CCR5^+CD4^+$ T cells. Additionally, such mAb administration inhibited the mobilization of NK cells and plasmacytoid dendritic cells characteristically seen in the control animals during acute infection accompanied by the inhibition of the synthesis of MIP-3α by the gut tissues. These data in concert suggest that blocking of GI trafficking $CD4^+$ T cells and inhibiting the mobilization of cell lineages of the innate immune system may be a powerful new tool to protect GI tissues and modulate acute lentiviral infection.

One of the hallmarks of HIV-1 infection of humans and natural or experimental SIV infection of nonhuman primates is that the virus primarily targets GALT during acute infection (1, 2). The targeting of GALT during acute infection occurs regardless of whether infection is via the sexual (mucosal) or the i.v. route (drug abuse related) and is reasoned to be due to the presence of large numbers of a highly susceptible CCR5-expressing activated $CD4^+$ T cells (3). The activated state of the $CD4^+$ T cells within the GALT has been reasoned to be due to the presence of these cells at the unique crossroads between microbial flora within the lumen and the epithelial cell lining of the gastrointestinal tissues (GIT)

Address correspondence and reprint requests to Dr. Aftab A. Ansari, Department of Pathology and Laboratory Medicine, Room 2309 WMB, Emory University School of Medicine, 101 Woodruff Circle, Atlanta, GA 30322. pathaaa@ emory.edu.

Disclosures The authors have no financial conflicts of interest.

The online version of this article contains supplemental material.

providing a source for constant antigenic exposure. Such targeting of the GIT by HIV/SIV leads to severe local $CD4^+$ T cell loss and mucosal tissue dysfunction (4) and is reasoned to be the basis for the "leaky gut syndrome" (5), which promotes bacterial translocation (6, 7) and chronic immune activation reminiscent of events that to a large extent parallel those noted during acute graft-versus-host (8) and chronic inflammatory bowel disease.

The fact that events that occur during the acute infection period basically dictate the kinetics of viral replication and the rate of disease progression in both HIVand SIV infection suggests that the detailed understanding of the initial dialogue that occurs between host and virus during the acute infection period may provide answers to the question of how and when immune dysfunction is initiated (9, 10). Knowledge derived from such studies is reasoned to provide important clues that could be incorporated in the formulation of an effective vaccine against HIV, which must target these early events. These findings underscore the potential important role the innate immune system must play during this acute infection period prior to the development of a mature adaptive immune response against the virus and virus-infected cells (11). These findings also dictate the need for a thorough understanding of the GIT, the cell lineages that are present in the GALT during normal physiology, and how these are altered following HIV/SIV infection. Additionally, the biology of the cells that comprise the GIT and the progenitor cells that replace such cell lineages either locally or by mobilization from the vasculature to the GALT and the effect that HIV/SIV infection has on these events are important issues that need to be addressed.

In this regard, it was the seminal studies during the late 1970s that documented the finding that lymphoid cells isolated from the skin or mucosal tissues home back to the tissue sites from which they were isolated (12). This finding paved the way for establishing the science of lymphocyte homing and trafficking. Since then, there have been many detailed studies that have provided insights into the various steps involved in lymphoid cell trafficking, which include the processes of adhesion, rolling, tethering, and diapedesis, as well as the role of specific cell surface molecules expressed by specific cell lineages that guide this process, and which are reviewed elsewhere (13–21). Thus, lymphoid cells have been shown to obtain environmental cues in the form of vitamins A, D3, and E, each of which induces them to express distinct cell surface molecules that direct them to specifically home either to the skin and cutaneous tissues or to the gastrointestingal (GI) tissues (13, 19). Although the precise chain of events continues to be defined, in the case of the gut-homing cells, it is clear that the $\alpha4\beta7$ integrin heterodimer and CCR9 expressed by lymphoid cells and their cognate ligands MAdCAM and CCL25 expressed by gut epithelial cells have been shown to attract and immobilize cells from the periphery and secondary lymphoid organs (SLOs) to the gut (15, 19, 22). Thus, vitamin A absorbed by the gut is metabolized into retinoic acid by appropriate enzymes when needed via the interaction between resident $CD103^+$ dendritic cells and gut or SLO stromal cells. Retinoic acid signaling following binding to its receptor on lymphoid cells leads to the upregulation of the $\alpha4\beta7$ integrin and CCR9 expression (14, 15), which promotes binding to their cognate receptors MAdCAM and CCL25, respectively, expressed on endothelial and gut epithelial cells, leading to their adhesion, extravasation, and homing to the gut tissues. Interestingly, epithelial cells lining the small intestine but not large intestine secrete CCL25 along a gradient that is highest at the proximal end (duodenum) and lowest at the distal end (ileum) (21), providing suggestive evidence that while the interaction between $\alpha4\beta7$ and MAdCAM serves to anchor lymphoid cells both in the small and large intestine, the interaction between CCR9 and CCL25 is likely restricted to the small intestine. There have been several reports that have documented differences in the cellular and molecular composition between the colon and small intestine (23–27), supporting the view that the host response in these two locations is likely to be different.

The findings that α4β7 integrin can serve as a receptor and signaling molecule for HIV and SIV and thus promote the upregulation of LFA-1 and cell-to-cell spread and in addition facilitates the trafficking of virus-infected cells from the periphery and SLOs to the gut (28) highlighted the potential importance of this gut-homing molecule. Furthermore, the report that most TH17$^+$ CD4$^+$ T cells express α4β7 and that α4β7-expressing CD4$^+$ T cells with a resting memory phenotype serve as the dominant target of SIV infection during acute infection (29) further emphasized the important role of α4β7-expressing CD4$^+$ T cells, particularly during the acute infection period. The relatively recent recognition that HIV prevention studies need to target the earliest stage of HIV/SIV infection to be effective (9, 10), coupled with the above-noted importance of α4β7-expressing CD4$^+$ T cells, prompted our laboratory to determine the potential outcome of in vivo targeting the α4β7 integrin with a novel recombinant rhesus mAb (30) during acute infection. Results obtained suggest that the administration of such an anti-α4β7 mAb to adult rhesus macaques just prior to and at 28 d after SIV infection delays the kinetics, reduces plasma viral loads (VLs), and markedly reduces viremia and proviral DNA load in the GALT. To our knowledge, this is the first study that suggests a beneficial role of inhibiting the potential GI trafficking of α4β7-expressing cells in SIV-infected animals and has important therapeutic implications.

Materials and Methods

Animals

This study included a total of eight adult female rhesus macaques weighing 8–10 kg housed at the Yerkes National Primate Research Center of Emory University. The animals used were specifically selected to be Mamu-A01, -B08, and -B17 negative in efforts to minimize the role of these MHC genes in conferring genetic control of viremia. The housing, care, diet, and maintenance were in conformance with the guidelines of the Committee on the Care and Use of Laboratory Animals of the Institute of Laboratory Animal Resources, National Research Council, and the Department of Health and Human Services guidelines titled Guide for the Care and Use of Laboratory Animals. All procedures involving studies using these animals were approved by the Emory Institutional Animal Care and Use Committee prior to the initiation of the studies. Each of these eight animals was negative for SIV, simian T cell lymphotropic virus, and simian retrovirus and was shown to have normal baseline immune and hematological values. The animals were divided into two groups of four animals each with four being administered the anti-α4β7 mAb and the other four serving as controls.

Administration of recombinant anti-α4β7 mAb

The rhesus recombinant monoclonal anti-α4β7 mAb was derived from a mouse mAb, which has been previously shown to have specificity for the α4β7 integrin heterodimer (31, 32) and consists of rhesus IgG1 and κ constant regions. The i.v. administration of a single dose of 50 mg/kg anti-α4β7 mAb to adult rhesus macaques has been previously shown by our laboratory to maintain plasma levels >10 μg/ml for 28 d (30). There was no detectable toxicity or changes in values of standard hematological, biochemical, and standard battery of kidney and liver function tests noted and was therefore considered safe. Based on these initial findings, each of the four rhesus macaques was i.v. administered 50 mg/kg sterile anti-α4β7 mAb on day −3 prior to SIV infection and a similar i.v. dose on day 28 postinfection (p.i.).

Virus used for infection

Each of the eight animals was injected i.v. with two hundred 50% tissue culture-infective doses of a single lot of SIVmac239 in a volume of 1 ml sterile PBS (pH 7.4). The virus stock

was prepared using day 3 PHA-P blasts of CD8-depleted PBMCs from unrelated rhesus macaques and stored under liquid nitrogen until use.

Mononuclear cell isolation from the blood and biopsy tissues

Besides the samples obtained in EDTA for VL determination, blood samples were also obtained at varying intervals in heparin and used for the studies reported in this article, which included polychromatic analysis of lymphoid cell subsets, proviral DNA loads, and measurement of mRNA levels for a number of transcription factors and cytokines. Colorectal and jejunal biopsies were obtained from each of the eight monkeys at baseline and then at weeks 1, 2, 3, 4, 10–12, and 19–23 p.i. An aliquot of the biopsies was used for the measurement of mRNA levels for a number of transcription factors and selected cytokines, and the rest was used for isolation of mononuclear cells that were used for levels of viral RNA, proviral DNA load determination, and flow analysis of lymphoid cell subsets. The optimized protocol for isolation of mononuclear cells from the biopsy tissues has been published elsewhere (30). The yields and viability of the pooled cells extracted from the biopsy tissues varied considerably, giving us a minimum of 0.3×10^6 to 3×10^6 total cells per sampling from each monkey, of which >70% were mononuclear. The viability ranged from 62 to 84% as determined by trypan blue dye exclusion technique. Lymph node biopsies were obtained during weeks 2 and 4 following infection. A single-cell suspension of the lymph node cells was prepared and used for the studies outlined.

Plasma VLs and cellular proviral determinations

Aliquots of EDTA plasma were obtained from all eight monkeys prior to and at varying intervals following SIV infection and sent on dry ice to Siemens Laboratories (Siemens, Berkeley, CA) for quantitating plasma SIV levels using the branched DNA assay. Data obtained are illustrated as plasma VL per milliliter of plasma. For the quantitation of proviral DNA load, aliquots of the unfractionated PBMCs and cells obtained from either the jejunal or colorectal gut biopsy tissues collected at various times postinfection were used to isolate total genomic DNA using the Qiagen DNAeasy kit (Qiagen, Valencia, CA). An aliquot of the genomic DNA isolated was used to quantitate the amount of DNA per sample, and the number of viral copies per nanogram of DNA was determined using our standardized laboratory protocol for quantitation of SIV gag (33, 34). The SIV1C cell line that has a single copy of SIV DNA per cell was used as a control for the proviral DNA analysis. The sensitivity of the assay was determined to be one infected cell per million. The quantitation of viral RNA was performed using RNA extraction, RNAse free primer pairs, and real-time PCR utilizing SYBR Green for iCycler kit as previously described (35). The sensitivity of this assay was determined to be 10 viral copies/ml.

Polychromatic flow cytometric analyses

Heparinized peripheral blood samples from each of the eight monkeys prior to anti-α4β7 mAb administration (three baseline value determinations) and at varying intervals thereafter were layered over Ficoll-Hypaque and, following centrifugation, cells at the interface were collected and subjected to polychromatic flow analysis. Each of the mAbs used had been previously screened to ensure its reactivity with cells from rhesus macaques and standardized panels were developed to identify subsets of CD4, CD8, NK, B, myeloid dendritic cells (mDCs), and plasmacytoid dendritic cells (pDCs). Various fluorochrome-conjugated Abs were used in appropriate combinations to derive the data that are illustrated in *Results*. The mAbs purchased from BD Biosciences (San Jose, CA) and used (with clone numbers in parentheses) included CD3 (SP34-2), CD4 (L200), CD8 (SK1), CD11c (S-HCL-3), CD14 (M5E2), CD16 (3G8), CD20 (2H7), CD28 (CD28-2), CD49d (L25), CD56 (NCAM16.2), CD95 (DX2), CD107A (LAMP-1), CD123 (7G3), CD161 (DX12), CD195-CCR5 (3A9), CD196-CCR6 (11A9), CD197-CCR7 (3D12), CD199-CCR9 (112509),

integrin β_7 (FIB504), HLA-DR (L243), and Ki67 (556027). The mAbs purchased from Miltenyi Biotec (Auburn, CA) and used included CD25 (4E3), FOXP3 (3G3), IL-12 (8.6), and IFN-α (LT27:295).

The mAbs purchased from Beckman Coulter (Brea, CA) and used included CD127 (R34.34), CD8b (CD8β), CD159a-NKG2a (Z199), CD314-NKG2d (ON72), CD337-NKp30 (Z25), and CD335-NKp46 (BAB281). The mAbs purchased from R&D Systems (Minneapolis, MN) and used included CD197-CCR7 (150503) and IL-23R (218213). The mAb purchased from eBioscience (San Diego, CA) and used was IL-17A (eBi64-CAP17). The protocol used for staining and data analysis, including the protocol used for intracellular staining of cytokines and CD107a and for the analysis of anti-α4β7 mAb-coated cells, has been published elsewhere (30). A total of a minimum of 10,000 events were analyzed to determine the frequency of each subset (except in the case of the analysis of mDCs and pDCs, in which a minimum of 100,000 events were analyzed) using FlowJo software, and the CBC values were used to calculate the absolute numbers of each cell lineage. Unfortunately, we could not obtain sufficient mononuclear lymphoid cells isolated from the gut biopsy specimens to accurately quantitate the frequencies of mDCs and pDCs.

For the detection of the α4β7 integrin in either PBMCs or GIT-obtained mononuclear cell samples prior to and after SIV infection, an aliquot of these cells was stained with PE-anti–α4 integrin, PE-Cy5 anti-β7 integrin, PE-Cy7 anti-CD4, allophycocyanin anti-α4β7, Alexa 700 anti-CD3, and PacBlue anti-CD8. Gated populations of $CD3^+$ (for all T cells) and $CD3^-$ (for all other cell lineages) were analyzed for the frequency of $CD3^+$ and $CD3^-$ cells that stained with α4β7 and coexpressed α4, α4β7 and coexpressed β7 or α4 and coexpressed β7 mAbs as outlined in Fig. 1*C*. A similar analysis was conducted on gated populations of $CD4^+$ and $CD8^+$ T cells. The failure to detect β7 but not α4 was taken as evidence of complete blocking of the α4β7 heterodimer and the fraction of cells thereof. Our findings showed complete blocking of the β7 and the α4β7 for at least 8 wk in all tissues examined and most of the tissues for up to 10–12 wk p.i. This strategy allowed us to determine the frequency of total T cells and non-T cells that expressed α4β7, total $CD4^+$ and $CD8^+$ T cells that express α4β7, and those from each of these lineages whose α4β7 was blocked.

Quantitative mRNA analysis

RNAwas isolated from aliquots of PBMCs or mononuclear cells isolated from the jejunal and colorectal biopsy tissues using the Qiagen RNAeasy Mini kit as per the manufacturer's instructions. The RNA was reverse transcribed using the Sigma-Aldrich enhanced avian kit (Sigma-Aldrich, St. Louis, MO). Aliquots of the cDNA were used to quantitate the relative levels of a number of transcription factors using the TaqMan primer pairs and probe and the 96-well assay system (StepOnePlus real-time PCR assay; Applied Biosystems, Carlsbad, CA). The transcription factors analyzed included primer pairs and probe either specific for rhesus macaques or human reagents known to cross-react with rhesus macaques and included rhesus FOXP3 (Rh02788830-m1), rhesus GARP (LRRC32, Rh02916124-m1), rhesus IL-17A (Rh026221759-m1), rhesus T-bet (TBX21, Rh02621772-m1), human GATA3 (Hs00231122-m1), and human RORC (Hs01076112M1). The Applied Biosystems kits use the rhesus β_2-microglobulin (Rh02847367-m1) as the reference. The data were analyzed using the software provided by the manufacturer and were used to derive values for net threshold cycle (C_T; using the β_2-microglobulin as a reference), and the values obtained from the baseline samples from the same monkey to calculate net values expressed as ΔΔCT. Additionally, levels of mRNA specific for rhesus IL-21, IL-22, IL-23, CCL-20, and for purposes of reference GAPDH were also quantitated using the SYBR Green real-time PCR assay using the following primer pairs: 5′-TGTGAATGACTTGGACCCTGAA-3′ and 5′-AAACAGGAAATAGCT GACCACTCA-3′ for IL-21; 5′-TCCGCGGAGTCAGTATGAGTGAGC-3′ and

GAACCTATCCGATTGAGGGAGC AGC-3′ for IL-22; 5′-GGACAACAGTCAGTTCTGCTT-3′ and 5′-CACAGGGCTATCAGGCAGC-3′ for IL-23p19; 5′-ACCATGTG CTGTACCAAGAGTTTG-3′ and 5′-CTAAACCCTCCATGATGTGCAAGTGA-3′ for CCL20 (MIP-3α); and 5′-GCACCACCAACTGCTTAGCAC-3′ and 5′-TCTTCTGGGTGGCAGTGATG-3′ for GAPDH. The values for IL-21, IL-22, IL-23, and CCL20 were expressed relative to the values for GAPDH, and the ratios obtained with the baseline values were used to calculate the fold increases. For the purpose of brevity, data from the four animals in each of the two groups were used to calculate mean ± SD values, and only the mean values are shown. The SD for each datum point was <15%. Additionally, only data from the jejunal biopsies are shown. The data obtained on the colorectal biopsy tissues showed basically similar trends but a larger degree of variation in the values (between 14 and 32%).

Measurement of plasma levels of anti-α4β7 mAb and anti-Ig Abs

A flow cytometry-based assay employing the human $CD4^+$ HuT 78 cell line was used to quantitate plasma levels of anti-α4β7 mAb as previously described (30). The same plasma samples were also assayed for monkey anti-α4β7 mAb Abs. Ninety-six–well plates were coated overnight with 100 μl/well anti-α4β7 mAb at 0.01 mg/ml in PBS and then blocked with Super Block (Thermo Scientific, Waltham, MA) for 15 min. Plasma samples were serially diluted in PBS/2% FBS and applied to the plates for 1 h. Plates were then washed 10 times with PBS/0.05% Tween and incubated for 1 h with biotinylated goat anti-human λ-chain (Miltenyi Biotec, Bergisch Gladbach, Germany). This Ab cross-reacts with rhesus λ L chain but does not recognize the recombinant anti-α4β7 Ab administered to the monkeys, which has κ L chains. Wells were then washed 10 times with PBS/0.05% Tween and incubated for 1 h with streptavidin-HRP (Invitrogen). After 10 more washes with PBS/0.05%Tween, plates were incubated for 3 min with peroxidase substrate solution (Kirkegaard & Perry Laboratories, Gaithersburg, MD). TMB stop solution (Kirkegaard & Perry Laboratories) was then added to each plate and OD was read on an ELISA plate reader at 450 nm. A sample was considered positive at a given dilution if the OD reading of the post-treatmentt plasma exceeded the OD of the pretreatment at the same dilution by 2-fold.

Statistical analysis

For each treated and control animal, plots were constructed to depict observed trajectories over time with respect to each measured quantity. Specifically, plasma VL (copies/ml) and jejunal viral and colorectal RNA load (copies/ng) were each plotted on a base $\log_{10}$ scale. Proviral DNA loads (copies/ng DNA) in sequential jejunal and sequential colorectal biopsies were plotted on an absolute scale, as were the numbers of pDCs (absolute number/μl blood). Median levels at the identified peak time points were compared across the treated and control groups via a standard nonparametric Wilcoxon rank sum test. In the case of plasma VL levels, trajectories for each animal on the base $\log_{10}$ scale were approximately linear from week 6 onward. Additional analysis of these log-transformed longitudinal VL levels from weeks 6–17 was undertaken by means of a mixed effects linear model (36), allowing for distinct intercepts and slopes across the two groups while accounting for within-animal correlation. Standard statistical tests based on this model were used to compare the slopes and week 6 intercepts across groups.

Results

Expression of α4β7 integrin on lymphoid cell subsets in the blood, jejunal, and colorectal tissue biopsies following infusion of anti-α4β7 mAb

As outlined in *Materials and Methods*, four rhesus macaques were each administered 50 mg/kg anti-α4β7 mAb i.v. on day −3, infected with SIVmac239 on day 0, and injected with the

same dose and route of the anti-α4β7 mAb on day 28 p.i. This dose of anti-α4β7 mAb administration was well tolerated clinically. Four additional rhesus macaques were similarly infected and served as controls. Plasma samples obtained at varying intervals after anti-α4β7 mAb administration were monitored for levels of the infused Ab. As seen in Fig. 1*A*, plasma levels >10 μg/ml were maintained for 4 wk after the first infusion and 4–6 wk after the second infusion. Plasma samples were also assayed for the induction of monkey anti-α4β7 mAb and shown to be negative (<1:10) throughout the observation period (data not shown), confirming the low immunogenicity of this recombinant Ab.

Aliquots of PBMCs, lymph node cells, and mononuclear cells isolated from the jejunal and colorectal biopsies prior to and at varying intervals after i.v. infusion of anti-α4β7 mAb and SIV infection of the four monkeys were analyzed for the expression of the α4β7 heterodimer. The objective of this analysis was to monitor the kinetics by which the administration of the mAb results in either depletion of the targeted α4β7-bearing cells or binding to the α4β7 heterodimer. Although all of the major cell lineages were monitored, data presented in this study are focused on the $CD4^+$ T cells since they are the major target of SIV infection. Representative data as displayed in Fig. 1*B* show that while a significant frequency of $CD4^+$ T cells from the PBMCs, jejunal, and colorectal biopsy tissues and lymph node cells obtained prior to anti-α4β7 mAb administration expressed α4β7, cells from the same tissues obtained as early as day 3 p.i. for PBMCs, week 2 p.i. for the lymph node cells, and week 1 p.i. for the mononuclear cells from the colorectal and jejunal biopsy tissues (the earliest time point sampled) showed virtually no binding of the anti-α4β7 Ab (31) for cells from each of the four animals. The inability to detect the α4β7 heterodimer-expressing cells was also noted in cells from other tissues and for each of the other cell lineages (data not shown), and this effect was maintained for at least 8 wk after SIV infection in each of the tissues from the four Ab-treated animals. These findings suggest that the dose of the anti-α4β7 mAb infused was sufficient to result in binding site saturation for 8 wk, which would cover the entire acute SIV infection period.

Two lines of data support the view that the anti-α4β7 mAb did not deplete $\alpha4\beta7^+$ lymphocytes. For the first, we took advantage of the fact that while the in vivo anti-α4β7 mAb treatment blocked the subsequent in vitro detection of the β7-chain, it does not block the detection of the α4-chain. Thus, as seen in Fig. 1*C*, the Abs we employed for flow cytometry could readily detect the α4 integrin on $CD4^+$ T cells in the post-treatmentt PBMC samples at the same frequency as samples from the baseline studies. This suggests that the α4β7-expressing $CD4^+$ T cells are likely to be coated (blocked) by the anti-α4β7 mAb and not deleted. Second, while all four anti-α4β7 mAb-treated animals showed a biphasic increase in the absolute number of $CD4^+$ T cells expressing CCR9 (the other gut-homing marker) following SIV infection, each of the four control animals showed a depletion of the $CCR9^+CD4^+$T cell subset (Fig. 1*D*). These data reconfirm the preferential targeting of the α4β7 and CCR9 gut-homing cells by SIV as previously documented (37) and they show that the administration of the anti-α4β7 mAb protects this subset from depletion; furthermore, the data are consistent with our previously published finding that the anti-α4β7 mAb is a nondepleting Ab (30). These data in concert document the fact that the i.v. administration of the anti-α4β7 mAb leads to nearly complete blocking of the α4β7 heterodimer on all tissues examined for up to until at least 8 wk p.i.

Effect of in vivo anti-α4β7 mAb infusion on plasma, jejunal, and colorectal VLs

VLs were monitored in each of the eight rhesus macaques post SIV infection. As seen in Fig. 2*A*, there were clear differences in the profile noted in the two groups of monkeys. First, there was a delay (about a week) in the detection of peak plasma viremia in each of the four animals that received the anti-α4β7 mAb as compared with the control animals. Second, there was a marked difference in the level ($p = 0.021$) and timing of peak viremia

and VL set point in the monkeys that received the anti-α4β7 mAb (Fig. 2*A*) as compared with the controls. Thus, while all four of the monkeys that received the anti-α4β7 mAb reached median peak levels of ~4 × 10^6 copies/ml plasma, the values for the controls were ~8-fold higher (median peak levels, >32 × 10^6/ml plasma). Additionally, whereas three of four of the anti-α4β7 mAb-treated animals showed VL set point of <100,000 copies/ml plasma with two of four having plasma VL of <13,000 copies/ml plasma at week 19 p.i., three of four control monkeys showed a log higher set point VL of >1,000,000 copies/ml plasma. The VL decline 6 wk p.i. and beyond also showed statistical difference in the $\log_{10}$ VL slope between the α4β7-treated monkeys and the controls ($p = 0.028$). When the VLs were analyzed in the context of corresponding values of absolute numbers of peripheral blood $CD4^+$ T cells, as seen in Fig. 2*B*, the differences in the plasma VLs appear to be even more marked. The monkeys receiving the anti-α4β7 mAb showed peak levels at week 3 as compared with the control monkeys that appeared to show an earlier peak. Thus, decreases in the absolute numbers of $CD4^+$ T cells accompanied by higher plasma VLs translate into high VL per $CD4^+$ T cells in the control animals and vice versa. SIV VL was also quantitated in mononuclear cells isolated from the jejunal and colorectal biopsies. As seen in Fig. 2*C* and 2*D*, an important pattern emerged. Thus, the jejunum appear to have relatively lower VL than did the colorectal tissues in both the anti-α4β7 mAb-treated and the control animals. These data need to be interpreted in the context of the differences in the number of lymphoid cell aggregates that are present at much higher levels in the colorectal tissues as compared with the jejunal and small bowel tissues. Thus, we routinely obtained a much higher yield of mononuclear cells isolated from the colorectal biopsies than an equivalent amount of jejunal tissue biopsies. Second, the administration of the anti-α4β7 mAb markedly reduced median peak viral RNA levels in both the jejunal and colorectal tissues in each of the four animals (range, 72–188 copies/ng RNA for jejunal tissues and 148–212 copies/ng RNA for the colorectal tissues) as compared with the four control animals (range, 3346–5243 for the jejunal tissues and 15,000–22,000 copies/ng RNA in the colorectal tissues; $p = 0.021$ for both jejunal and colorectal values).

Effect of in vivo anti-α4β7 mAb infusion on proviral DNA load in PBMCs and mononuclear cells from jejunal and colorectal biopsies

The levels of proviral DNA were analyzed in both PBMCs and mononuclear cells isolated from the colon and jejunum from the four monkeys that received the anti-α4β7 mAb and were compared with levels in similar tissue samples from the four control monkeys. We purposely used unfractionated mononuclear samples for these analyses since we did not know whether the treatment of the animals with the anti-α4β7 mAb may promote infection of other cell lineages. In the anti-α4β7–treated animals (Fig. 3*A*), low but detectable levels of proviral DNA (copies/ng DNA) were first seen in the PBMCs as early as 1 wk p.i. with a gradual and progressive increases at week 2 (10–24 copies/ng DNA) and week 3 (8–46 copies/ng DNA), after which levels decreased. In contrast, the pattern in the control animals was not as clear with values lower than those from the anti-α4β7 mAb-treated animals, potentially a reflection of rapid emigration of infected cells from the blood. Thus, while two of four control animals showed proviral DNA in PBMC samples at weeks 1 and 2, somewhat stable levels appeared at week 3 and thereafter decreased.

In contrast to blood, levels of proviral DNA were consistently lower in sequential GI tissues from the anti-α4β7–treated monkeys as compared with controls (Fig. 3*B*, 3*C*) and there were generally lower levels in the jejunal tissues than in the colorectal tissues. Please see earlier comments concerning one of the contributing factors for such small versus large bowel differences. There was also a markedly lower level of proviral DNA in the jejunal (peak median level, 1.72 copies/ng DNA) and colorectal biopsy tissues (peak median level, 0.84 copies/ng DNA) f6rom the anti-α4β7 mAb-treated animals than from the controls

(peak median values, 6.57 copies/ng DNA for the jejunal tissues and 10.71 copies/ng DNA for the colorectal tissues, with $p = 0.021$ for both jejunal and colorectal values). The values peaked at 3 wk p.i. and then declined gradually thereafter in both groups of animals; importantly, whereas all four animals in the anti-α4β7 mAb-treated group eventually showed undetectable level of integrated virus, animals in the control groups still maintained low but detectable levels at months 4–5 p.i. These data suggest that the administration of the anti-α4β7 mAb markedly reduces the level of viremia and the frequency of provirus-infected resident $CD4^+$ T cells within the GI tissues during acute viremia.

Effect of anti-α4β7 mAb administration on the major lymphoid cell lineages in the blood

Aliquots of PBMCs from each of the four animals administered the anti-α4β7 mAb and the four control animals were subjected to polychromatic flow cytometric analysis using multiple panels of mAbs. Data on only those specific for $CD4^+$ T cells and their subsets and selected innate immune cell lineages (because the study covers the acute infection period) are shown. The data for the baseline values for all eight animals in this study are the means of three determinations made prior to the initiation of the anti-α4β7 mAb administration. Data presented show values for absolute numbers of each cell lineage based on the corresponding lymphoid cell count.

As seen in Fig. 4*A*, whereas the absolute numbers of CD4 counts generally decrease in each of the four control animals from a range of 572–1772 at baseline to a range of 256–751 by week 2 p.i. and a range of 111–193 at week 10 p.i., the values in the anti-α4β7 mAb-treated animals increased. Thus, whereas the baseline values in the anti-α4β7 mAb-treated animals ranged from 721 to 1494, the values for week 2 p.i. were 1041–2118 and the values for week 10 were 968 1296. Of interest is that even at week 28 p.i. while each of the control animals showed a continuing decline in the absolute CD4 counts, the values in the anti-α4β7 mAb-treated animals at week 28 p.i. continued to be maintained similar to the values at week 10. These findings clearly suggest that the administration of the anti-α4β7 mAb significantly prevents the depletion and/or redistribution of $CD4^+$ T cells in the blood by mechanisms that are not clear at present. When the subsets of $CD4^+$ T cells were analyzed, as seen in Fig. 4*B–D*, it appears that there is an initial decrease in the absolute numbers of the naive and effector memory $CD4^+$ T cells in both the control and the Abtreated group with a trend toward an increase in at least 2 of 4 animals that received the anti-α4β7 mAb at 6 mo p.i. However, the major difference between the control and the Ab-treated animals was reflected in the absolute numbers of the central memory $CD4^+$ T cell subset. Overall, changes in the number of central memory $CD4^+$ T cells followed a pattern similar to that seen with the total $CD4^+$ T cell numbers, with an increase at week 2 and at weeks 8–10 p.i. However, these data also suggest that the administration of the anti-α4β7 mAb may lead to a selective increase of the central memory $CD4^+$ T cell subset. Because the CCR5-expressing $CD4^+$ T cells are the major target of infection and depletion, the absolute numbers of this subset in the PBMCs were also monitored in the eight monkeys.

As seen in Fig. 5*A*, whereas there is a gradual depletion of this subset in each of the four control animals starting at about week 3 p.i., which continues to decrease as a function of time, there appears to be a recovery of the $CD4^+CCR5^+$ subset in the anti-α4β7 mAb-treated animals by week 6, which is thereafter maintained even in the presence of significant plasma VLs (see Fig. 2*A*). These data suggest that during the period of achieving VL set point, there is either a marked difference in the relative susceptibility of the $CD4^+CCR5^+$ subset in these two groups of animals or a very robust turnover rate of this cell lineage. In efforts to determine which of the $CD4^+$ T cell subsets was actively proliferating, the frequency of $Ki67^+$ cells within the naive, effector memory (EM), and central memory (CM) $CD4^+$ T cell subsets from each of the eight animals was determined. As seen in Fig. 5*B*, while the naive $CD4^+$ T cells from the anti-α4β7 mAb-treated animals showed a gradual

increase in the levels of $Ki67^+$ naive $CD4^+$ T cells, which peaked ~4–6 wk p.i., the control animals had significantly smaller increases. The major increase in Ki67-expressing $CD4^+$ T cells occurred in the CM $CD4^+$ T cell subset (see Fig. 5*C*; note the difference in scale) but only in the animals that received the anti-α4β7 mAb. This increase was maintained until months 4–5, after which the numbers declined to baseline levels. The numbers of $Ki67^+$ CM $CD4^+$ T cells in the control animals, in contrast, showed decreases. Importantly, the increase in Ki67-expressing CM $CD4^+$ T cells in the anti-α4β7 mAb-treated animals did not occur early but ~4–6 wk p.i. and was probably unrelated to the direct effects of the Ab treatment. There appeared to be an initial decline in the number of $Ki67^+$ cells within the EM $CD4^+$ T cell subset followed by increases in some but not all of the animals (see Fig. 5*D*), with increases being more marked in the animals that received the anti-α4β7 mAb. The number of $CD4^+$ T cells that expressed CD25 (an activation marker) on $CD4^+$ T cells (Fig. 5*E*) showed a trend of increasing numbers in the anti-α4β7 mAb-treated animals starting 2–3 wk p.i. In contrast, this subset decreased in the control animals. A number of additional markers expressed by $CD4^+$ T cells were also analyzed but failed to show differences and/or distinct trends in the two groups of animals. These included analysis of the frequency of $CD4^+$ $CD25^{hi}/FOXP3^+$ (regulatory T cells) and $CD4^+$ T cells that expressed PD-1 (data not shown). These data in concert suggest that the administration of the anti-α4β7 mAb protects the $CD4^+$ T cells from infection/depletion. However, the higher levels of proliferating ($Ki67^+$) $CD4^+$ T cells and activated $CD25^+$-expressing $CCR5^+CD4^+$ T cells seem at odds with lower plasma VLs in these animals, suggesting that proliferation and activation appear to be disconnected from viral infection and replication, suggesting a re-evaluation of an accepted dogma. These findings also suggest that in addition to activation, $CD4^+$ T cell traffic may be critical for optimal viral replication. The effect of anti-α4β7 mAb administration on the other cell lineages was also studied and showed complete blocking of the α4β7 heterodimer (data not shown). Additionally, the numbers of CD8 α/β T cells and their subsets were also examined (Supplemental Fig. 1). As seen, in general, treatment of the monkeys with the anti-α4β7 mAb mutes the effect virus infection has on this cell lineage at least during the acute infection period as reflected by regulating lower increases in a number of the $CD8^+$ T cell subsets, which correlates with lower VLs.

Effect of anti-α4β7 mAb administration on $CD4^+$ and $CD8^+$ T cells in jejunal and colorectal biopsy tissues

It is clear that analysis of cells from biopsy tissues needs to be interpreted with caution, as the methods that are used are far from optimal. Nonetheless, we did isolate cells pooled from several either jejunal or colorectal biopsies and analyzed them primarily for determining whether the anti-α4β7 mAb treatment was efficient in reaching these tissues. Studies therefore focused on the frequencies of $CD3^+CD4^+$ and $CD3^+CD8^+$ T cells that expressed the α4β7 integrin prior to and after infection. The profile for α4β7 integrin expression by the cells from each of the jejunal and colorectal tissues from the anti-α4β7 mAb-treated group examined (from week 1 to 10) was similar to that seen in Fig. 1 with complete blockage (data not shown). Note the presence of a significantly higher frequency ($p = 0.021$) of $CD4^+$ T cells in the anti-α4β7 mAb-treated group than in the control group (Fig. 6) but markedly lower levels of viral RNA (Fig. 2*C*, 2*D*) and proviral DNA (Fig. 3*C*, 3*D*). Additionally, overall, a couple of interesting observations were made. First, the total number of mononuclear cells isolated from the colorectal tissues was 3- to 10-fold higher than from the same amount of jejunal tissue. Second, the frequencies of $CD4^+$ T cells and the CD4/CD8 ratio were slightly higher in the colorectal tissues than in the jejunal tissues at baseline in each of the eight animals. As seen in Fig. 6, the frequencies of $CD4^+$ T cells increased by weeks 1 and 2 in both the jejunal and colorectal tissues of the anti-α4β7 mAb-treated group. Thereafter, the frequency of $CD4^+$ T cells was maintained to baseline levels in the jejunal tissues up to week 10 but declined at week 10 in the colorectal tissues. In contrast, the

frequencies of α/β $CD8^+$ T cells was either maintained or showed marked increases in both jejunal and colorectal tissues from all four of the anti-α4β7 mAb-treated group. In contrast, whereas there were similar numbers of $CD4^+$ and $CD8^+$ T cells in the baseline jejunal and colorectal biopsies of the control group as seen with the anti-α4β7 mAb-treated group, there was a rapid depletion of nearly all $CD4^+$ T cells within 1 wk p.i. and a concomitant increase in the frequencies of $CD8^+$ T cells. Depletion of $CD4^+$ T cells postinfection to ultra-low levels in the control group precluded analysis of α4β7 expression by $CD4^+$ T cells from the control group. Taken together, these data indicate that the administration of the anti-α4β7 mAb protects the jejunal tissue resident $CD4^+$ cells more than the colorectal tissue resident $CD4^+$ T cells as compared with similar $CD4^+$ T cells from the control group and blocks the detection of the α4β7 integrin. Additionally, there appears to be increased numbers of $CD8^+$ T cells entering both the jejunal and colorectal tissues.

Effect of anti-α4β7 mAb administration on cell lineages of the innate immune system

Because the studies reported in this article primarily involved analysis conducted on cells and tissues collected during the acute infection period, when the innate immune system is reasoned to be performing its function, it was our objective to characterize the effect of anti-α4β7 mAb administration on NK cells and the two major dendritic cell subsets, the pDCs and mDCs, in the peripheral blood and the GI tissues. The strategy to define NK cells and their subsets have been detailed elsewhere (35, 38). Results of the studies on NK cells in the blood showed that whereas two of four of the control monkeys show marked increases and the other two showed moderate gradual increases in the absolute numbers of $CD3^-$, CD8 α^+, $NKG2a^+$, $CD16^+$, $CD56^-$ cells (the cytolytic NK cell subset) up to 8 wk p.i., none of the monkeys treated with the anti-α4β7 mAb showed such increases (see Fig. 7*A*). The absolute numbers of this cytolytic NK cell subset in the control group thereafter decreased somewhat. The pattern for the $CD3^-$, CD8 α/α^+, $NKG2a^+$, $CD16^-$, $CD56^+$ cells (the noncytolytic cytokine-synthesizing NK cell subset) was basically similar to that seen with the cytolytic subset (Fig. 7*B*) in the same individual monkeys, denoting that the increases appear to affect both of the major NK cell subsets in the control group and that treatment with the anti-α4β7 mAb muted the increases in each of these subsets.

When the effects of anti-α4β7 mAb administration on the levels of mDCs and pDCs were analyzed, as seen in Fig. 8*A*, whereas each of the animals from the two groups show a gradual decline in the absolute numbers of mDCs, the decrease appeared more profound in the control group as compared with the anti-α4β7 mAb-treated animals. Of importance was the finding of a major difference in the kinetic changes in the absolute numbers of pDCs in the two groups. Thus, as seen in Fig. 8*B*, whereas there is an early sharp increase (week 1, $p = 0.021$) in the absolute number of pDCs in the control group (peak median value, 9.85 pDCs/μl), this increase was not noted in any of the anti-α4β7 mAb-treated animals and the values remained stable (week 1, median value, 2.9 pDCs/μl). Once again, whereas the absolute numbers of pDCs gradually declined in both groups, the decrease appeared more profound in the control group.

With respect to innate immune cells among the mononuclear cells isolated from the jejunal and colorectal tissues, a small frequency (0.5–1%) of NK cells was noted in the baseline samples from either the jejunal or colorectal tissues. Of these NK cells, most were $CD16^-$, $CD56^+$ (range, 52–68%), the rest either were $CD16^+$, $CD56^+$ or $CD16^-$, $CD56^-$ (15–25% double-positive double-negative each). Of interest, a very low frequency of these NK cells was $CD16^+$, $CD56^-$ (the major cytolytic subset). The level of α4β7 expression on these NK cells from baseline tissues was distinctly lower than the NK cells from the baseline PBMC samples. While the frequencies of each of these NK cell subsets did not change significantly following SIV infection in the anti-α4β7 mAb-treated group, there clearly was a significant increase (from 1.7 to 3.1%) in the control group (data not shown). In these samples we failed

to detect significant frequencies of mDCs pDCs in cells harvested from any of the eight animals at baseline. However, there was clearly a significant increase in the frequencies of pDCs in the control animals but not the anti-α4β7 mAb-treated animals after SIV infection (data not shown). However, the limited numbers of cells (due to the low yields) precluded acquiring data amenable to statistical analysis. Data obtained levels of mRNA for IFN-α and IRF-7 from the same tissues, however, showed a marked increase in the levels of these two molecules in RNA from mononuclear cells, but only in the control group, not in the anti-α4β7 mAb-treated group (data not shown), supporting the view that there was an increase in the infiltration pDCs (a major source of IFN-α) localized to the jejunal and colorectal biopsy tissues. We hypothesize that this infiltration gut tissues by NK cells and pDCs was inhibited by treating the animals with the anti-α4β7 mAb, which has important significance for the gut-associated pathogenesis in SIV-infected animals.

Effect of anti-α4β7 mAb administration on selected cytokines and transcription factors

Aliquots of mononuclear cells from jejunal and colorectal biopsies were analyzed for relative levels of mRNA coding for FOXP3 and GARP (as indicators of regulatory T cells) and for IL-17A and RORC2 (as indicators of Th17 cells). Additionally, levels of mRNA coding for the cytokines IL-21, IL-22, and IL-23 (due to their role in influencing GI immune interactions) and the relative levels of MIP-3α (CCL20, gut chemokine involved in recruitment) were also measured. As seen in Fig. 9*A*, besides values for GARP, the cells from the jejunal biopsies from the anti-α4β7 mAb-treated group showed no change in the levels of mRNA coding for FOXP3, IL-17A, RORC2, IL-21, IL-22, and MIP-3α and a slight increase in IL-23 during the acute infection period (up to week 10 p.i.) and then a sharp decline in IL-17A, RORC2, IL-21, IL-22, and IL-23 at 4 mo p.i. In contrast, the mRNA isolated from the control group showed a sharp initial increase (FOXP3, GARP, IL-21, IL-23, and MIP-3α) or a sharp decrease (IL-17A, RORC2, and IL-23) during the acute infection period. The values for each of these thereafter decreased and stayed low thereafter. The changes in values obtained on the colorectal tissues from the control and anti-α4β7 mAb-treated group for GARP, IL-17A, RORC2, and IL-23 were essentially similar to those seen in the jejunal biopsies. However, the values for the other molecules showed some differences. Thus, there appeared to be sharp decrease in values for FOXP3 and slight increases in values for IL-21, IL-22, IL-23, and MIP-3α. The significance of these differences between jejunal and colorectal tissues could be secondary to differences in the number of lymphoid cell aggregates that are present in higher numbers in the latter tissues. Of interest was the finding of the almost complete blocking of MIP-3α synthesis in the jejunal tissues and markedly lower levels in the colorectal tissues from the α4β7-treated animals as compared with marked increase in the control animals during acute infection, which is consistent with our hypothesis that CCL20 upregulation leads to the recruitment of pDCs into the gut mucosa and remarkably anti-α4β7 mAb treatment blocks the synthesis of CCL20 and reduces the infiltration of pDCs into the gut tissues. These data in concert appear to suggest that whereas the control group shows a marked increase in the proinflammatory response within the gut tissues, this proinflammatory response is muted in the gut tissues of the anti-α4β7 mAb-treated group.

Discussion

To better understand the role of the α4β7 integrin during acute SIV infection, we administered a rhesus recombinant form of an Ab targeting this integrin molecule to a group of SIV-infected rhesus macaques. Two administrations maintained plasma levels of >10 μg/ml of the Ab for the first 8 wk of SIV infection. What is not clear is whether the Ab administered was able to reach “all” of the target tissues in an effective manner, particularly the GALT, which comprises 70% of all lymphoid cells in the body as compared with

peripheral blood, which represents only 2% of the total lymphoid cells (39). The finding of nearly complete blocking of the α4β7 integrin on cells isolated from all of the tissues examined, including the jejunal and colorectal biopsies of the anti-α4β7 mAb-treated animals, suggests that such therapy was quite effective (see Fig. 1*B*). The mechanisms by which the in vivo administration of anti-α4β7 mAb delayed and decreased plasma and gut tissue viremia and proviral DNA loads in both the jejunal and colorectal mononuclear cells is clearly one of the major issues that needs to be addressed. Thus, the issues include whether such mAb administration depletes the cells following binding, inhibits the trafficking of the α4β7-expressing (presumably activated) $CD4^+$ T cells to the gut tissues (minimizing the so-called adding fuel to the fire), or reduces the ability of the virus to infect the putative major target cells in blood and the various tissues and thus reduces the cell-to-cell spread (by inhibition of the activation of LFA-1) (28) and transport of virus and virus-infected cells to the gut tissues, the major site of acute viral replication.

The isotype of the recombinant rhesus Ab used in this study is an IgG1, which was chosen because this isotype was considered to have the highest cytolytic potential. However, as seen in the data presented in this article (Fig. 1), this mAb was clearly not lytic. Thus, it is difficult to think that use of another isotype of Ab such as IgG4 (known to have noncytolytic function) would provide any difference. Importantly, however, perhaps use of a Fab fraction would have a deeper tissue distribution. With regard to whether the mAb functioned by blocking virus binding versus trafficking, it is difficult at present to distinguish between these two possibilities since evidence for the ability of the anti-α4β7 mAb to function by inhibiting trafficking and binding of the virus to the cells both exist. It has already been established that the anti-α4β7 mAb is directed at a conformational epitope of the α4β7 molecule and does not recognize either the α4- or β7-chain alone (40). The anti-α4β7 mAb also not only specifically binds but also selectively inhibits the adhesion of the α4β7 heterodimer to MAdCAM-1 (32). Thus, the fact that the anti-α4β7 mAb does not bind or inhibit the adhesion of the α4β1 or αEβ7 heterodimers to their cognate ligands suggests an element of high specificity. Additionally, the α4-chain of the α4β7 heterodimer has previously been shown to contain the principal sequences involved in the binding of the heterodimer to MAdCAM-1, its cognate ligand (41). The anti-α4β7 mAb used in the studies reported in this article in addition to a number of other mAbs with specificity for the α4-chain were shown to inhibit the binding of HIV gp120 to the α4β7 heterodimer (28). The fact that the binding of these mAbs with specificity for the α4-chain was localized to residues 152–203 of the α4-chain (42) suggests that the anti-α4β7 mAb potentially inhibits the binding of HIV and by inference SIV to the heterodimer preventing viral entry, activation of LFA-1, inhibition of the formation of the virological synapse, and limiting viral spread. The fact that the anti-α4β7 mAb binds to similar motifs as the mAb with specificity for the α4-chain, which are involved in binding to MAdCAM-1, also supports the view that the administration of the anti-α4β7 mAb must inhibit trafficking of the $CD4^+$ T cells to the gut tissues. In this regard, note the molecular constraints placed by the binding of the anti-α4β7 mAb to cells that express this heterodimer. Thus, as defined by Arthos et al. (28), while the recognition specificity of the anti-α4β7 mAb lies on the α4-chain of the heterodimer, it appears that the addition of the anti-α4β7 mAb to cells blocks the binding of mAb against the β7-chain but not the α4-chain (see Fig. 1*B*). The finding of markedly reduced VLs in both the jejunal and colorectal tissues from the anti-α4β7 mAb-treated animals as compared with the control animals, coupled with the finding of the presence of significant numbers of $CD4^+$ T cells in these tissues in the presence of high levels of circulating virus, also suggests that such mAb treatment inhibits the infection of these gut-resident $CD4^+$ T cells likely by inhibiting the carriage of virus by virus-infected cells or conferring resistance to the $CD4^+$ T cells present in the gut. It is thus difficult at present to determine whether such lower VLs in the GI tract is due to decreased trafficking or local inhibition by binding of the α4β7 integrin expressed by the $CD4^+$ T cells. Future tracking

studies utilizing tagged anti-α4β7 mAb are needed in efforts to determine the normal physiological trafficking of these cells and the effect SIV has on modulating such trafficking. It is also important to remember that while the gut mucosae are considered to be highly susceptible to HIV/SIV infection and replication, the fact that peak viremia is coincident with $CD4^+$ T cell depletion suggests that other tissues besides the gut may be the major source of plasma viremia (43). Importantly also, binding of the envelope protein gp120 of not only HIV-1 but also SIVsmm shares the tripeptide motif (residues 182–184) that has been shown to bind to the α4β7 integrin (30). These findings suggest that both HIV-1 and SIV interact with the α4β7 integrin in the same fashion and the mAb inhibits the binding of both HIV-1 and SIV isolates.

Importantly, in the normal physiological setting, activation of T cells has been shown to lead to phosphorylation of the intracellular sequences of integrins, including the integrin β7, and such phosphorylation is thought to lead to the generation of an “activated” form of the integrin that promotes its binding to its cognate ligand (44), a process termed “inside out” signaling. Thus, it is not clear at present whether ligation of the α4β7 molecule by mAb leads to a similar activation of intracellular pathways that include “cross talk” with other molecules involved in T cell activation that may play a role in the relative resistance of these cells to infection by SIV. The finding of an increase in the number of $CD4^+$ T cells that are $Ki67^+$, but considerably later after the administration of the anti-α4β7 mAb (see Fig. 5*C*), suggests that the Ab does not directly induce activation and proliferation. The higher frequencies of sustained levels of CD25-expressing $CD4^+$ T cells support this view (see Fig. 5*E*). Clearly, the integrins including the heterodimeric α4β7 integrin have functions in addition to adhesion. In this regard, note that a linkage of integrin activation with pathways of T cell activation has previously been documented (44). The fact that anti-α4β7 mAb administration leads to the maintenance of a significantly higher frequency of $CD4^+$ T cells that express CCR5 (see Fig. 5*A*) than in the control animals, but with a much lower VL, suggests that factors other than the frequency of CCR5-expressing $CD4^+$ T cells contribute to differences in the levels of plasma viremia. This finding is reminiscent of the finding of a lack of correlation between the frequencies of CCR5-expressing $CD4^+$ T cells and plasma VLs in the natural hosts of SIV infection (45) and the finding of a lack of correlation between flow cytometric-based levels of CCR5 expression and the frequency of virus-infected memory $CD4^+$ T cells in the gut tissues of SIV-infected monkeys (37). Nevertheless, although anti-α4β7 mAb treatment of the animals reduces VL, there are still significant levels of viremia in these animals and the source of this viremia would be important to identify. Thus, it was previously reasoned that the GALT was the major source of plasma viremia. However, the data presented show the presence of a markedly lower level of viral RNA and a marked decrease in the frequency of proviral DNA containing cells in the jejunal and colorectal biopsies of the anti-α4β7 mAb-treated animals, providing suggestive evidence that the virus maybe replicating elsewhere in these animals. Along these lines, also note that there appeared to be relatively higher levels of virus in the colorectal as compared with jejunal tissues from the same animal. Although a number of features that distinguish colorectal from jejunal tissues of the GI tract have been documented (21, 23–27), it could be that the difference in VL could merely reflect the number of $CD4^+$ T cells that are localized to these two tissue sites within the GI tract. Chief among the differences between these two anatomic locations within the GI tract is the finding of the expression of CCL25, the ligand for CCR9 that has been shown to be expressed along a gradient with the highest level at the proximal end (duodenum) and lowest level at the distal end (ileum) of the small intestine (21). Thus, it is reasoned that CCR9 expression is dispensable for trafficking of cells to the large intestine but likely plays an important role in trafficking of cells to the small intestine. The fact that there was a higher VL in the colorectal as compared with jejunal tissues of the animals treated with the anti-α4β7 mAb is thus difficult to understand. It would seem that cells could alternatively use CCR9 and traffic into the small

intestine even though the α4β7 integrin was blocked and thus contribute to a relatively higher homing and infiltration of the $CD4^+$ T cells to the jejunum than the large intestine. It is possible, however, that the expression of CCL25 could have been downregulated by the administration of the anti-α4β7 mAb, and since the expression of CCL25 is required for the activation of CCR9 so that it can function to bind to CCL25 and induce the trafficking of the cells to the small intestine, this process could have been inhibited. Future studies aimed at defining the levels of CCL25 in the gut tissues of the animals treated with the anti-α4β7 mAb are planned.

Results of the studies reported in this article also document the many direct/indirect effects of the administration of the anti-α4β7 mAb on changes in the frequency and absolute numbers of subsets of various lineages of lymphoid cells in the peripheral blood. The mechanisms that lead to such changes and their impact on the pathogenesis of SIV infection are important to define. Table I summarizes these changes. Thus, anti-α4β7 mAb administration clearly induces expansion of naive and CM $CD4^+$ T cells. The control animals, in contrast, show a gradual progressive decline in absolute number of $CD4^+$ T cells, a hallmark of pathogenic SIV infection. Although it is reasonable to assume that the biphasic increase in $CD4^+$ T cells in the anti-α4β7 mAb-treated animals is secondary to the ability of the anti-α4β7 mAb to induce $CD4^+$ T cell activation, the kinetics of the response puts this view into question. Thus, as seen in Fig. 4*A*, there is actually an initial decline (when there are high levels of circulating anti-α4β7 mAb) in absolute CD4 T cell counts in three of four animals at week 1, and the peak increase only occurs at week 2 in all four animals followed by a second peak between weeks 8 and 10. Thus, there is a delay of 2 wk following the first administration and a delay of 4–6 wk after the second administration of the mAb when such peak values were observed. Note that there is also an increase in the absolute numbers of CD8α/β TCR-expressing cells that roughly coincides with the increases seen in the $CD4^+$ T cells in the anti-α4β7 mAb-treated animals, which may also be secondary to the same mechanisms. These increases of the CD8 subset are distinguished from the peak increases that occur at 4–5 wk in the control animals. These data seem to imply that these increases in the anti-α4β7 mAb-treated as compared with the control animals are likely due to the activation of different pathways. Importantly, in this regard, note that the α4β7 integrin is either expressed constitutively or induced to express following activation of not only subsets of $CD4^+$ and $CD8^+$ T cells, but also by B cells (46), macrophages (47), NK cells (48, 49), dendritic cells (50), and mast cells (51). Thus, this integrin serves as a general mucosal homing marker for a variety of hematopoietic cells. The administration of the anti-α4β7 mAb therefore likely has the potential to inhibit the trafficking of most if not all of these lineages if the appropriate chemokine is synthesized and these lineages express the appropriate receptor. It is also possible that ligation of the α4β7 molecule on cells of one of these other lineages such as the dendritic cell lineages and macrophages leads to the generation of cytokines and chemokines that induce the proliferation of the $CD4^+$ and $CD8^+$ T cells noted in the current study. This view would be consistent with the increases seen in the expression of Ki67 and CD25 by the $CD4^+$ T cells (Fig. 5*C*, 5*E*). Studies are in progress to define the potential nature of the cytokines induced by the in vivo administration of the anti-α4β7 mAb. Also, note the increases in subsets that occur in the control animals but that either are not seen or are quantitatively less in the anti-α4β7 mAb-treated animals. Thus, some of the highlights of these changes in the $CD8^+$ T cell lineage include a marked increase in the number of $CD8^+$ T cells expressing CCR5, a steady high level of CD25 expression, and an increase in the FOXP3-expressing $CD8^+$ T cells. The CCR5 molecule has been shown to promote extravasation and trafficking of cells to sites of inflammation and infection (40), indicating that the $CD8^+$ T cells, particularly the subset that express α4β7, are destined to localize to the mucosal tissues of the control animals in response to SIV infection. Presumably, therefore, anti-α4β7 mAb treatment either inhibits the mobilization of CCR5-expressing $CD8^+$ T cells or inhibits the expression of the CCR5 molecule on $CD8^+$

T cells in the anti-α4β7 mAb-treated animals. The fact that this increase in CCR5-expressing cells was seen in the CD8 cells but not in the $CD4^+$ T cell lineage of the control animals (see Fig. 5*A*) suggests that CCR5 expression is differentially regulated, confirming previously published findings that there are distinct mechanisms involved in CCR5 expression by $CD8^+$ T cells as compared with $CD4^+$ T cells (52). In this regard, note that chief among the various cytokines that have been shown to induce CCR5 expression is IFN-α (53). It is thus tempting to speculate that the inhibition of pDC mobilization as noted in the anti-α4β7 mAb-treated animals (Fig. 8*B*) may have led to decreased levels of IFN-α, resulting in decreased frequencies of CCR5-expressing $CD8^+$ T cells. The pathways involved in the transcriptional regulation of FOXP3 expression continue to be defined, and whether they are the same within $CD4^+$ and $CD8^+$ T cells has not been addressed. While the expression of FOXP3 has been associated with the combined signaling induced via TCR, IL-2, and TGF-β and the integration of these signals by a network of intracellular signaling molecules including PI3K, protein kinase B, mTOR, and Foxo factors (54), its stable expression has been shown to require the binding of Ets-1 to the demethylated FOXP3 gene (55). The level at which α4β7 interferes with these pathways remains to be established.

The changes in cell lineages involved in the execution of innate immune response are of central interest for the studies reported in this article since the studies primarily cover the period of acute infection. Two of the cell lineages that were studied carefully included the NK and DC lineages. As seen in Fig. 7*A* and *B*, there appears to be a marked increase in the absolute numbers of the two major subsets (cytolytic and cytokine synthesizing) of NK cells in all four of the control animals but none of the anti-α4β7 mAb-treated animals. In fact, there was also a similar increase in the $CD16^-/CD56^-$ (double-negative) subset. The rapid increase in the NK cells shortly after SIV infection of rhesus macaques has been previously documented by our laboratory (35). In efforts to determine the mechanism by which treatment with anti-α4β7 mAb treatment inhibits this rapid increase, it was reasoned that studies aimed at defining whether this increase is due to fresh minting of NK cells from precursor cells in the bone marrow or mobilization from depots resident in other lymphoid tissues would be appropriate. Our failure to detect significant changes in the levels of the transcription factors (involved in NK cell differentiation) NFil-3a, Notch-L-Δ-4, and *Fms*-like tyrosine kinase-L (56, 57) at the mRNA level (data not shown) provides suggestive evidence that the increases were likely due to mobilization from other depots. The nature of the signals involved in mobilizing these NK cells has not yet been defined. These two major NK cell subsets share a number of chemokine receptors (CCR2, CXCR1, CXCR3, CXCR4) but also express chemokine receptors unique to each (such as CCR5 and CCR7 for the $CD16^-/CD56^+$ subset and CX3CR1, SIP5, and ChemR23 for the $CD16^+/CD56^-$ subset). Additionally, the cytokines IL-7 and membrane-bound form of IL-15 have been implicated in their activation and maturation (11). The analysis of these cytokines and chemokines in the plasma from the control and anti-α4β7 mAb-treated animals is actively being pursued. The sharp transient increase in the absolute numbers of pDCs and the progressive decreases in the absolute numbers of both mDCs and pDCs are also of great interest. Thus, pDCs are not expected to migrate in response to inflammatory stimuli (58), although they express high levels of CCR7. However, the ligation of CD40 expressed by pDCs leads to their maturation accompanied by activation of CCR7 into a functional chemokine receptor that responds to CCL19 the ligand for CCR7. It has been shown that such CCL19 ligation promotes the migration of pDCs to lymph nodes and secondary lymphoid organs. Ligation of CXCR4 on pDCs by CXCL12 also leads to the synthesis of CCL3 (MIP-1α) and promotes their migration to lymph nodes and secondary lymphoid organs. These findings led us to quantitate levels of CCL19 and MIP-1α in the plasma of the animals. We failed to detect significant differences in the levels of either CCL19 or MIP-1α (data not shown) and therefore reason that if there is an increase, this may occur earlier than the time point of the plasma samples we analyzed. It is of interest that while we failed to detect any significant

number of pDCs in the jejunal or colorectal biopsies from the control or anti-α4β7 mAb-treated animals at baseline (even following analysis of $>10^6$ events), there was clearly a low frequency of pDCs following SIV infection but only in the control animals, not in the anti-α4β7 mAb-treated animals (data not shown). Unfortunately, the limited cells harvested from the biopsies precluded us to derive sufficient number of events to make these data meaningful. Studies are currently in progress to obtain a larger number of cells from such gut biopsy tissues to determine not only their frequency but also whether these are pDC1 or pDC2 based on the intracellular detection of IL-10 and IL-17, respectively (59). However, the fact that we were able to observe readily detectable levels of mRNA for IRF-7 and IFN-α (pDCs are a major source of these) in the colorectal and jejunal biopsies of some of the control but not the anti-α4β7 mAb-treated animals (S. Kwa, personal communication) provides support to the view that there must be trafficking of pDCs to the gut tissues during pathogenic infection. The gradual decrease in both pDCs and mDCs in PBMCs are likely due to their homing to lymph nodes and secondary lymphoid organs. However, the levels of decrease seen were more marked in the control than in the anti-α4β7 mAb-treated animals, likely secondary to lower levels of viremia and lower levels of inflammation.

We hypothesize that shortly after SIV infection there is a rapid mobilization of α4β7 expressing not only gut homing $CD4^+$ T cells but also both NK cells and pDCs to the gut tissues in response to inflammation induced by SIV infection and replication. The depletion of massive amounts of $CD4^+$ T cells accompanied by damage to gut epithelial cells lining the gut tissues and a sustained proinflammatory innate immune response lead to irreversible pathology prior to the advent of adaptive immune responses. The regulation and timely control of these innate immune responses may be one of the keys to facilitate recovery of the gut immune system, allowing the development and execution of an effective virus-specific adaptive immune response. We submit that inhibiting the trafficking of not only $CD4^+$ T cells but also gut homing NK cells and pDCs may be instrumental in lowering gut pathology, maintaining CD4 levels, and lowering of VL. A more sustained administration of the anti-α4β7 mAb in conjunction with blocking of CCR9, the alternate gut-homing molecule, may provide a powerful new approach for the therapy of SIV and by implication human HIV-1 infection.

Supplementary Material

Refer to Web version on PubMed Central for supplementary material.

Acknowledgments

We thank Dr. Michael M. Lederman (Case Western Reserve University) and Dr. Ashley Haase (University of Minnesota) for critiques of the manuscript, Dr. Joseph J. Mattapallil (Uniformed Services University of the Health Sciences, Bethesda, MD) for advice, and Drs. Suefen Kwa and Rama Rao Amara (Emory University) for discussions in the conduct of this study. We also thank Stephanie Ehnert and staff at the Yerkes National Primate Center of Emory University for help in the care of the animals and for the timely procurement of samples and tissues for all of the studies reported in this article. We also thank Irene Dreith for technical assistance.

This work was supported by National Institutes of Health/National Institute of Allergy and Infectious Diseases Grant RO1 AI078773, National Institutes of Health/National Institute of Allergy and Infectious Diseases Contracts HHSN2722009000037C and R24 RR016001, Public Health Service Grant UL1 RRo25008, and Yerkes National Primate Research Center Base Grant NIH-DRR-00165.

Abbreviations used in this article

CM	central memory
C_T	threshold cycle

EM	effector memory
GI	gastrointestinal
GIT	gastrointestinal tissues
mDC	myeloid dendritic cell
pDC	plasmacytoid dendritic cell
p.i.	postinfection
SLO	secondary lymphoid organ
VL	viral load

References

1. Brenchley JM, Schacker TW, Ruff LE, Price DA, Taylor JH, Beilman GJ, Nguyen PL, Khoruts A, Larson M, Haase AT, Douek DC. $CD4^+$ T cell depletion during all stages of HIV disease occurs predominantly in the gastrointestinal tract. J. Exp. Med. 2004; 200:749–759. [PubMed: 15365096]
2. Veazey RS, DeMaria M, Chalifoux LV, Shvetz DE, Pauley DR, Knight HL, Rosenzweig M, Johnson RP, Desrosiers RC, Lackner AA. Gastrointestinal tract as a major site of $CD4^+$ T cell depletion and viral replication in SIV infection. Science. 1998; 280:427–431. [PubMed: 9545219]
3. Brenchley JM, Douek DC. HIV infection and the gastrointestinal immune system. Mucosal Immunol. 2008; 1:23–30. [PubMed: 19079157]
4. Paiardini M, Frank I, Pandrea I, Apetrei C, Silvestri G. Mucosal immune dysfunction in AIDS pathogenesis. AIDS Rev. 2008; 10:36–46. [PubMed: 18385779]
5. Douek D. HIV disease progression: immune activation, microbes, and a leaky gut. Top. HIV Med. 2007; 15:114–117. [PubMed: 17720995]
6. Brenchley JM, Price DA, Schacker TW, Asher TE, Silvestri G, Rao S, Kazzaz Z, Bornstein E, Lambotte O, Altmann D, et al. Microbial translocation is a cause of systemic immune activation in chronic HIV infection. Nat. Med. 2006; 12:1365–1371. [PubMed: 17115046]
7. Douek DC, Roederer M, Koup RA. Emerging concepts in the immunopathogenesis of AIDS. Annu. Rev. Med. 2009; 60:471–484. [PubMed: 18947296]
8. Brenchley JM, Price DA, Douek DC. HIV disease: fallout from a mucosal catastrophe? Nat. Immunol. 2006; 7:235–239. [PubMed: 16482171]
9. Haase AT. Targeting early infection to prevent HIV-1 mucosal transmission. Nature. 2010; 464:217–223. [PubMed: 20220840]
10. Shattock RJ, Haynes BF, Pulendran B, Flores J, Esparza J, Working Group convened by the Global HIV Vaccine Enterprise. Improving defences at the portal of HIV entry: mucosal and innate immunity. PLoS Med. 2008; 5:e81. [PubMed: 18384232]
11. Bostik P, Takahashi Y, Mayne AE, Ansari AA. Innate immune natural killer cells and their role in HIV and SIV infection. HIV Therapy. 2010; 4:483–504. [PubMed: 20730028]
12. McDermott MR, Bienenstock J. Evidence for a common mucosal immunologic system, I: Migration of B immunoblasts into intestinal, respiratory, and genital tissues. J. Immunol. 1979; 122:1892–1898. [PubMed: 448111]
13. Berdnikovs S, Abdala-Valencia H, McCary C, Somand M, Cole R, Garcia A, Bryce P, Cook-Mills JM. Isoforms of vitamin E have opposing immunoregulatory functions during inflammation by regulating leukocyte recruitment. J. Immunol. 2009; 182:4395–4405. [PubMed: 19299740]
14. Hammerschmidt SI, Ahrendt M, Bode U, Wahl B, Kremmer E, Förster R, Pabst O. Stromal mesenteric lymph node cells are essential for the generation of gut-homing T cells in vivo. J. Exp. Med. 2008; 205:2483–2490. [PubMed: 18852290]
15. Johansson-Lindbom B, Agace WW. Generation of gut-homing T cells and their localization to the small intestinal mucosa. Immunol. Rev. 2007; 215:226–242. [PubMed: 17291292]

16. Marelli-Berg FM, Cannella L, Dazzi F, Mirenda V. The highway code of T cell trafficking. J. Pathol. 2008; 214:179–189. [PubMed: 18161751]

17. Miles A, Liaskou E, Eksteen B, Lalor PF, Adams DH. CCL25 and CCL28 promote α4β7-integrin-dependent adhesion of lymphocytes to MAdCAM-1 under shear flow. Am. J. Physiol. Gastrointest. Liver Physiol. 2008; 294:G1257–G1267. [PubMed: 18308860]

18. Park EJ, Mora JR, Carman CV, Chen J, Sasaki Y, Cheng G, von Andrian UH, Shimaoka M. Aberrant activation of integrin α4β7 suppresses lymphocyte migration to the gut. J. Clin. Invest. 2007; 117:2526–2538. [PubMed: 17786243]

19. Sigmundsdottir H, Butcher EC. Environmental cues, dendritic cells and the programming of tissue-selective lymphocyte trafficking. Nat. Immunol. 2008; 9:981–987. [PubMed: 18711435]

20. Staton TL, Habtezion A, Winslow MM, Sato T, Love PE, Butcher EC. $CD8^+$ recent thymic emigrants home to and efficiently repopulate the small intestine epithelium. Nat. Immunol. 2006; 7:482–488. [PubMed: 16582913]

21. Stenstad H, Svensson M, Cucak H, Kotarsky K, Agace WW. Differential homing mechanisms regulate regionalized effector $CD8\alpha\beta^+$ T cell accumulation within the small intestine. Proc. Natl. Acad. Sci. USA. 2007; 104:10122–10127. [PubMed: 17551016]

22. Mora JR, von Andrian UH. Role of retinoic acid in the imprinting of gut-homing IgA-secreting cells. Semin. Immunol. 2009; 21:28–35. [PubMed: 18804386]

23. Agace WW. T-cell recruitment to the intestinal mucosa. Trends Immunol. 2008; 29:514–522. [PubMed: 18838302]

24. Apostolaki M, Manoloukos M, Roulis M, Wurbel MA, Müller W, Papadakis KA, Kontoyiannis DL, Malissen B, Kollias G. Role of β7 integrin and the chemokine/chemokine receptor pair CCL25/CCR9 in modeled TNF-dependent Crohn's disease. Gastroenterology. 2008; 134:2025–2035. [PubMed: 18439426]

25. Kaufman DR, Barouch DH. Translational Mini-Review Series on Vaccines for HIV: T lymphocyte trafficking and vaccine-elicited mucosal immunity. Clin. Exp. Immunol. 2009; 157:165–173. [PubMed: 19604255]

26. Mora JR. Homing imprinting and immunomodulation in the gut: role of dendritic cells and retinoids. Inflamm. Bowel Dis. 2008; 14:275–289. [PubMed: 17924560]

27. Wang C, Kang SG, HogenEsch H, Love PE, Kim CH. Retinoic acid determines the precise tissue tropism of inflammatory Th17 cells in the intestine. J. Immunol. 2010; 184:5519–5526. [PubMed: 20400707]

28. Arthos J, Cicala C, Martinelli E, Macleod K, Van Ryk D, Wei D, Xiao Z, Veenstra TD, Conrad TP, Lempicki RA, et al. HIV-1 envelope protein binds to and signals through integrin α4β7, the gut mucosal homing receptor for peripheral T cells. Nat. Immunol. 2008; 9:301–309. [PubMed: 18264102]

29. Kader M, Wang X, Piatak M, Lifson J, Roederer M, Veazey R, Mattapallil JJ. $\alpha4^+\beta7^{hi}CD4^+$ memory T cells harbor most Th-17 cells and are preferentially infected during acute SIV infection. Mucosal Immunol. 2009; 2:439–449. [PubMed: 19571800]

30. Pereira LE, Onlamoon N, Wang X, Wang R, Li J, Reimann KA, Villinger F, Pattanapanyasat K, Mori K, Ansari AA. Preliminary in vivo efficacy studies of a recombinant rhesus anti-$\alpha_4\beta_7$ monoclonal antibody. Cell. Immunol. 2009; 259:165–176. [PubMed: 19616201]

31. Lazarovits AI, Moscicki RA, Kurnick JT, Camerini D, Bhan AK, Baird LG, Erikson M, Colvin RB. Lymphocyte activation antigens, I: A monoclonal antibody, anti-Act I, defines a new late lymphocyte activation antigen. J. Immunol. 1984; 133:1857–1862. [PubMed: 6088627]

32. Soler D, Chapman T, Yang LL, Wyant T, Egan R, Fedyk ER. The binding specificity and selective antagonism of vedolizumab, an anti-α4β7 integrin therapeutic antibody in development for inflammatory bowel diseases. J. Pharmacol. Exp. Ther. 2009; 330:864–875. [PubMed: 19509315]

33. Mori K, Yasutomi Y, Sawada S, Villinger F, Sugama K, Rosenwith B, Heeney JL, Uberla K, Yamazaki S, Ansari AA, Rübsamen-Waigmann H. Suppression of acute viremia by short-term postexposure prophylaxis of simian/human immunodeficiency virus SHIV-RT-infected monkeys with a novel reverse transcriptase inhibitor (GW420867) allows for development of potent antiviral immune responses resulting in efficient containment of infection. J. Virol. 2000; 74:5747–5753. [PubMed: 10846052]

34. Villinger F, Brice GT, Mayne AE, Bostik P, Mori K, June CH, Ansari AA. Adoptive transfer of simian immunodeficiency virus (SIV) naive autologous $CD4^+$ cells to macaques chronically infected with SIV is sufficient to induce long-term nonprogressor status. Blood. 2002; 99:590–599. [PubMed: 11781243]
35. Pereira LE, Johnson RP, Ansari AA. Sooty mangabeys and rhesus macaques exhibit significant divergent natural killer cell responses during both acute and chronic phases of SIV infection. Cell. Immunol. 2008; 254:10–19. [PubMed: 18640666]
36. Laird NM, Ware JH. Random-effects models for longitudinal data. Biometrics. 1982; 38:963–974. [PubMed: 7168798]
37. Mattapallil JJ, Douek DC, Hill B, Nishimura Y, Martin M, Roederer M. Massive infection and loss of memory $CD4^+$ T cells in multiple tissues during acute SIV infection. Nature. 2005; 434:1093–1097. [PubMed: 15793563]
38. Jaroenpool J, Rogers KA, Pattanapanyasat K, Villinger F, Onlamoon N, Crocker PR, Ansari AA. Differences in the constitutive and SIV infection induced expression of Siglecs by hematopoietic cells from non-human primates. Cell. Immunol. 2007; 250:91–104. [PubMed: 18331725]
39. Pabst R, Russell MW, Brandtzaeg P. Tissue distribution of lymphocytes and plasma cells and the role of the gut. Trends Immunol. 2008; 29:206–208. author reply 209–210. [PubMed: 18394963]
40. Schweighoffer T, Tanaka Y, Tidswell M, Erle DJ, Horgan KJ, Luce GE, Lazarovits AI, Buck D, Shaw S. Selective expression of integrin α4β7 on a subset of human $CD4^+$ memory T cells with hallmarks of gut-trophism. J. Immunol. 1993; 151:717–729. [PubMed: 7687621]
41. Zeller Y, Mechtersheimer S, Altevogt P. Critical amino acid residues of the α4 subunit for α4β7 integrin function. J. Cell. Biochem. 2001; 83:304–319. [PubMed: 11573247]
42. Schiffer SG, Hemler ME, Lobb RR, Tizard R, Osborn L. Molecular mapping of functional antibody binding sites of α4 integrin. J. Biol. Chem. 1995; 270:14270–14273. [PubMed: 7782282]
43. Lay MD, Petravic J, Gordon SN, Engram J, Silvestri G, Davenport MP. Is the gut the major source of virus in early simian immunodeficiency virus infection? J. Virol. 2009; 83:7517–7523. [PubMed: 19458001]
44. Hilden TJ, Valmu L, Kärkkäinen S, Gahmberg CG. Threonine phosphorylation sites in the β2 and β7 leukocyte integrin polypeptides. J. Immunol. 2003; 170:4170–4177. [PubMed: 12682249]
45. Veazey R, Ling B, Pandrea I, McClure H, Lackner A, Marx P. Decreased CCR5 expression on $CD4^+$ T cells of SIV-infected sooty mangabeys. AIDS Res. Hum. Retroviruses. 2003; 19:227–233. [PubMed: 12689415]
46. Rott LS, Rosé JR, Bass D, Williams MB, Greenberg HB, Butcher EC. Expression of mucosal homing receptor α4β7 by circulating $CD4^+$ cells with memory for intestinal rotavirus. J. Clin. Invest. 1997; 100:1204–1208. [PubMed: 9276738]
47. Fernekorn U, Butcher EC, Behrends J, Hartz S, Kruse A. Functional involvement of P-selectin and MAdCAM-1 in the recruitment of α4β7-integrin-expressing monocyte-like cells to the pregnant mouse uterus. Eur. J. Immunol. 2004; 34:3423–3433. [PubMed: 15484189]
48. Pérez-Villar JJ, Zapata JM, Melero I, Postigo A, Sánchez-Madrid E, López-Botet M. Expression and function of α4/β7 integrin on human natural killer cells. Immunology. 1996; 89:96–104. [PubMed: 8911146]
49. Reeves RK, Evans TI, Gillis J, Johnson RP. SIV infection induces an expansion of $\alpha4\beta7^+$ and cytotoxic $CD56^+$ NK cells. J. Virol. 2010 10.1128/JVI.01126-10.
50. Saurer L, McCullough KC, Summerfield A. In vitro induction of mucosa-type dendritic cells by all-*trans* retinoic acid. J. Immunol. 2007; 179:3504–3514. [PubMed: 17785784]
51. Hallgren J, Gurish MF. Pathways of murine mast cell development and trafficking: tracking the roots and routes of the mast cell. Immunol. Rev. 2007; 217:8–18. [PubMed: 17498048]
52. Pett SL, Zaunders J, Bailey M, Murray J, MacRae K, Emery S, Cooper DA, Kelleher AD. A novel chemokine-receptor-5 (CCR5) blocker, SCH532706, has differential effects on $CCR5^+CD4^+$ and $CCR5^+CD8^+$ T cell numbers in chronic HIV infection. AIDS Res. Hum. Retroviruses. 2010; 26:653–661. [PubMed: 20560795]
53. Stoddart CA, Keir ME, McCune JM. IFN-α-induced upregulation of CCR5 leads to expanded HIV tropism in vivo. PLoS Pathog. 2010; 6:e1000766. [PubMed: 20174557]

54. Merkenschlager M, von Boehmer H. PI3 kinase signalling blocks Foxp3 expression by sequestering Foxo factors. J. Exp. Med. 2010; 207:1347–1350. [PubMed: 20603315]

55. Polansky JK, Schreiber L, Thelemann C, Ludwig L, Kruger M, Baumgrass R, Cording S, Floess S, Hamann A, Huehn J. Methylation matters: binding of Ets-1 to the demethylated Foxp3 gene contributes to the stabilization of Foxp3 expression in regulatory T cells. J. Mol. Med. 2010; 88:1029–1040. [PubMed: 20574810]

56. Haraguchi K, Suzuki T, Koyama N, Kumano K, Nakahara F, Matsumoto A, Yokoyama Y, Sakata-Yanagimoto M, Masuda S, Takahashi T, et al. Notch activation induces the generation of functional NK cells from human cord blood CD34-positive cells devoid of IL-15. J. Immunol. 2009; 182:6168–6178. [PubMed: 19414770]

57. Kamizono S, Duncan GS, Seidel MG, Morimoto A, Hamada K, Grosveld G, Akashi K, Lind EF, Haight JP, Ohashi PS, et al. Nfil3/E4bp4 is required for the development and maturation of NK cells in vivo. J. Exp. Med. 2009; 206:2977–2986. [PubMed: 19995955]

58. Penna G, Vulcano M, Sozzani S, Adorini L. Differential migration behavior and chemokine production by myeloid and plasmacytoid dendritic cells. Hum. Immunol. 2002; 63:1164–1171. [PubMed: 12480260]

59. Schwab N, Zozulya AL, Kieseier BC, Toyka KV, Wiendl H. An imbalance of two functionally and phenotypically different subsets of plasmacytoid dendritic cells characterizes the dysfunctional immune regulation in multiple sclerosis. J. Immunol. 2010; 184:5368–5374. [PubMed: 20357264]

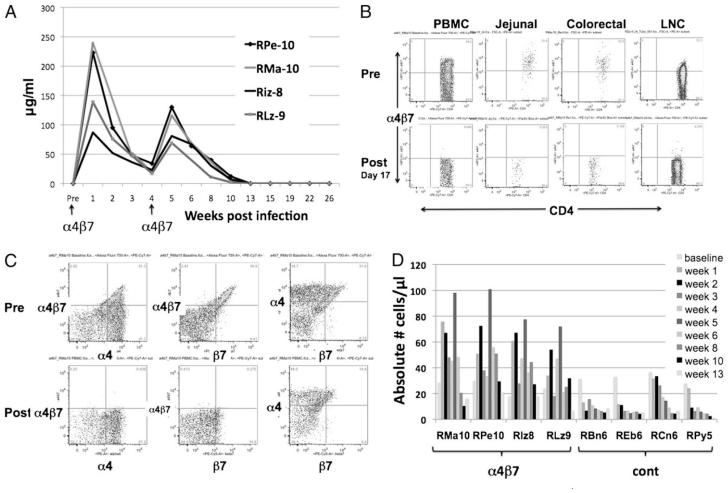

FIGURE 1.

In vivo quantitation of the plasma levels of the anti-α4β7 mAb and phenotypic characterization of $CD4^+$ T cells from SIV-infected rhesus macaques prior to and after administration of the anti-α4β7 mAb. *A*, Plasma samples from each of the four animals were assayed for levels of the mAb as described under *Materials and Methods*. *B*, Flow cytometric analysis of α4β7 expression by $CD4^+$ T cells from the PBMCs, jejunal, colorectal biopsies, and lymph nodes prior to and after anti-α4β7 mAb administration. Representative profiles of cells from one of the four animals prior to (*top*) and after (*bottom*) are depicted. These profiles were maintained until 10 wk p.i. Arrows indicate the time points when 50 mg/kg anti-α4β7 mAb was administered i.v. to each monkey. *C*, The anti-α4β7 mAb administration blocks the detection of this heterodimer on $CD4^+$ T cells. Representative flow cytometric profiles from one of the four animals administered the anti-α4β7 mAb are shown. The $CD3^+/CD4^+$-gated population of PBMCs was analyzed for the expression of the α4 integrin in combination with the α4β7 heterodimer (*left panels*), the β7 integrin in combination with the α4β7 heterodimer (*middle panel*), and the α4 integrin in combination with the β7 integrin (*right panels*) prior to (*top panels*) and after day 17 of anti-α4β7 mAb administration. *D*, Absolute numbers of CCR9-expressing $CD4^+$ T cells from the PBMCs of each of the four of the anti-α4β7 mAb-treated animals and each of the four control animals prior to and at varying intervals after anti-α4β7 mAb administration.

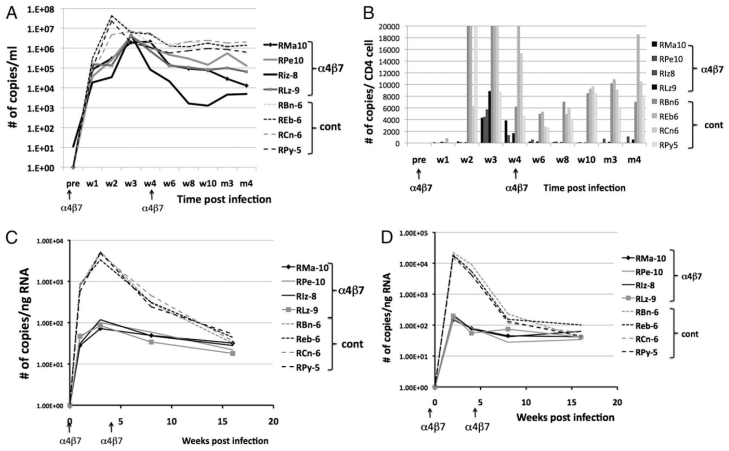

FIGURE 2.

Effect of anti-α4β7 mAb treatment on plasma, jejunal, and colorectal tissue viral RNA loads of SIV-infected rhesus macaques. Data depict the viral RNA loads in samples from each of the four monkeys treated with the anti-α4β7 mAb (solid lines or bars) and each of the four control animals (broken lines or light bars) in blood and tissues. *A*, Kinetics of plasma VL in the anti-α4β7 mAb-treated and control monkeys. The median peak values in the α4β7-treated versus control animals are statistically different ($p = 0.021$). *B*, Plasma VL calculated relative to the corresponding absolute $CD4^+$ T cell counts in blood. *C*, Number of viral RNA copies in cells isolated from the jejunal tissues expressed as copies per nanogram of RNA and (*D*) number of viral RNA copies in cells from the colorectal tissues expressed as copies per nanogram of RNA. The median peak values for plasma VL, jejunal, and colorectal VL in the α4β7-treated versus plasma VL, jejunal, and colorectal VL in the control animals are each statistically different ($p = 0.021$). The arrows at the bottom indicate the time of mAb administration. Note that the differences in the levels of viral RNA in the jejunal as compared with the colorectal tissues could be secondary to the presence of a larger number of lymphoid cell aggregates in the colorectal tissue biopsies as compared with the jejunal biopsies. We routinely isolated higher numbers of lymphoid cells from the colorectal than an equivalent number of jejunal tissue biopsies.

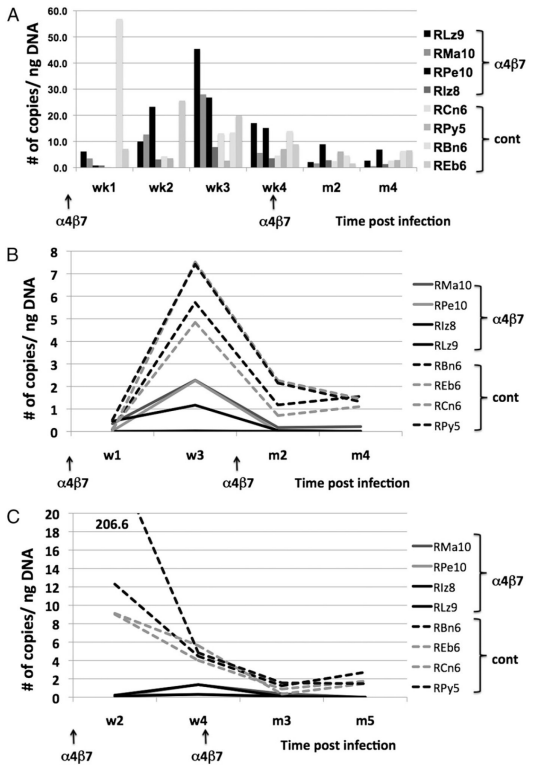

FIGURE 3.

Levels of proviral DNA expressed as copies per nanogram of DNA extracted from mononuclear cells from each of the four anti-α4β7 mAb-treated animals and the four control animals. Data shown are for samples from (*A*) PBMCs, (*B*) cells from the jejunal biopsies, and (*C*) cells from the colorectal biopsies. The peak levels of proviral DNA loads in the jejunal and colorectal tissues in the α4β7-treated animals are statistically different ($p = 0.021$) from the same tissues of the control animals. See caption for Fig. 2 for the potential reasons for the differences in the values obtained from the colorectal as compared with jejunal tissues.

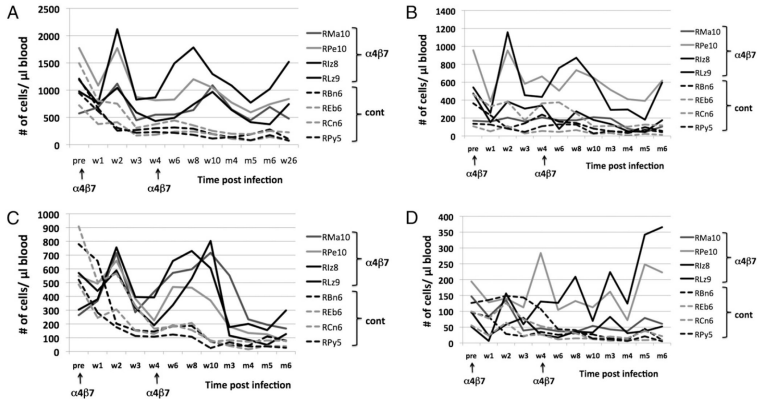

FIGURE 4.

Absolute numbers of peripheral blood $CD4^+$ T cells and its subsets in samples from the four anti-α4β7 mAb-treated animals (solid lines) and the four control animals (broken lines) at baseline and various time points after SIV infection. The arrows at the bottom indicate the times the anti-α4β7 mAb was administered. Data shown are for (*A*) total $CD4^+$ T cells, (*B*) naive $CD4^+$ T cells, (*C*) central memory $CD4^+$ T cells, and (*D*) effector memory $CD4^+$ T cells.

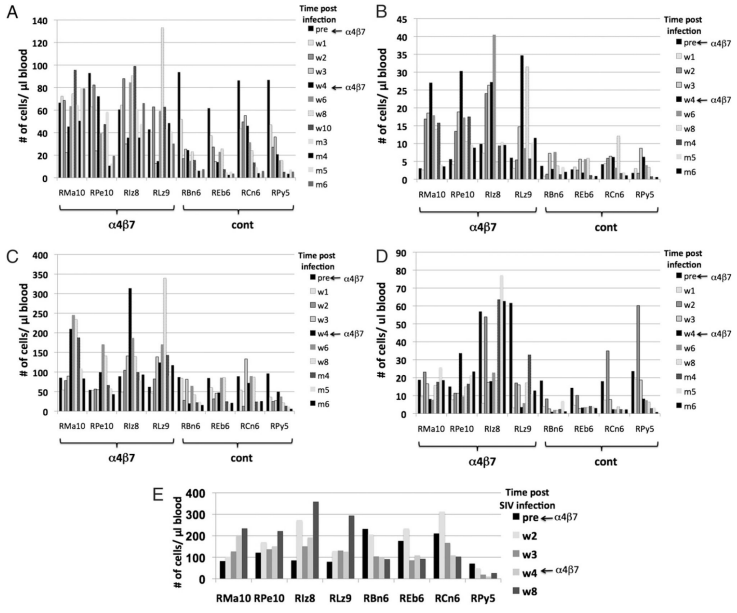

FIGURE 5.

Absolute numbers of CCR5-, Ki67-, and CD25-expressing $CD4^+$ T cell subsets in peripheral blood samples from the four α4β7 mAb-treated animals and the four control animals at baseline and various times after SIV infection. *A*, CCR5-expressing $CD4^+$ T cells, (*B*) $Ki67^+$ naive $CD4^+$ T cells, (*C*) $Ki67^+$ central memory $CD4^+$ T cells, (*D*) $Ki67^+$ effector memory $CD4^+$ T cells, and (*E*) CD25-expressing $CD4^+$ T cells.

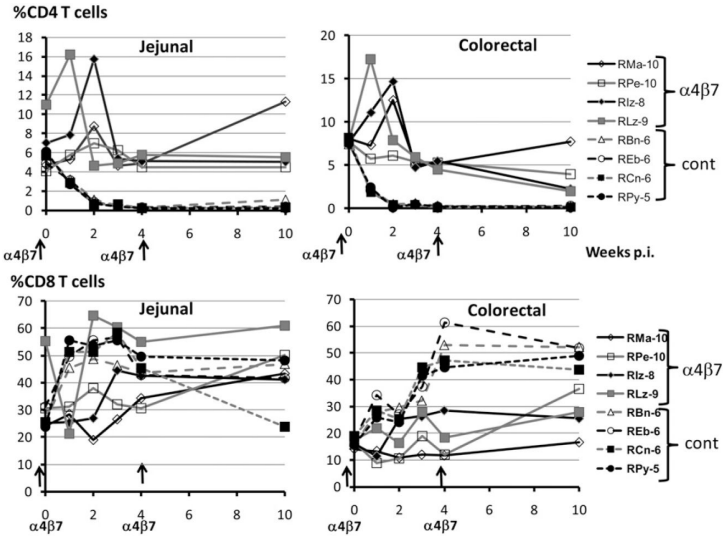

FIGURE 6.

Frequencies of $CD4^+$ (*top panels*) and $CD8^+$ T cells (*bottom panels*) in mononuclear cells isolated from pools of jejunal (*left panels*) and colorectal biopsies (*right panels*) from the four anti-α4β7 mAb-treated animals (solid lines) and the four control animals (broken lines) prior to (baseline) and after SIV infection.

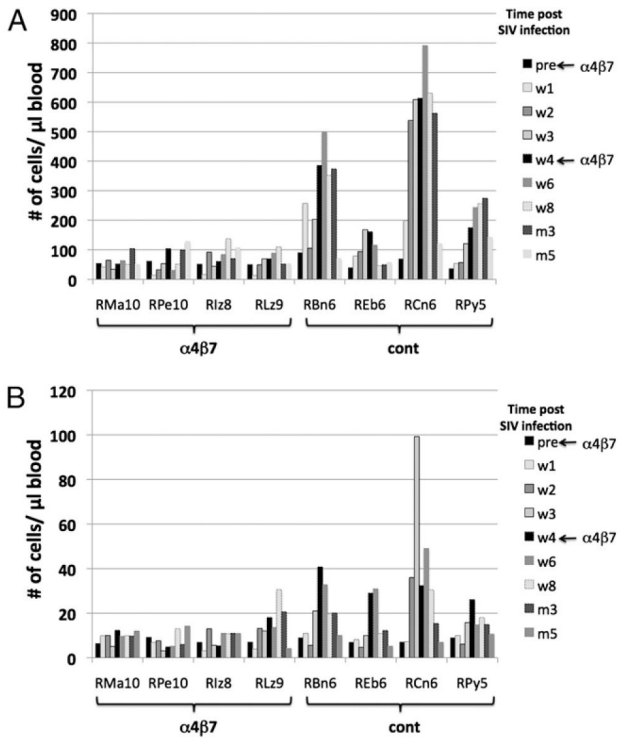

FIGURE 7.

Absolute numbers of the NK cells subsets in the four rhesus macaques treated with the anti-α4β7 mAb (*left panel*) and the four control animals (*right panel*). Data shown include absolute numbers of $CD3^{-}$, CD8 α/α^{+}, $NKG2a^{+}$ gated populations of (*A*) $CD16^{+}$, $CD56^{-}$ cytolytic subset and (*B*) $CD16^{-}$, $CD56^{+}$ cytokine synthesizing subset.

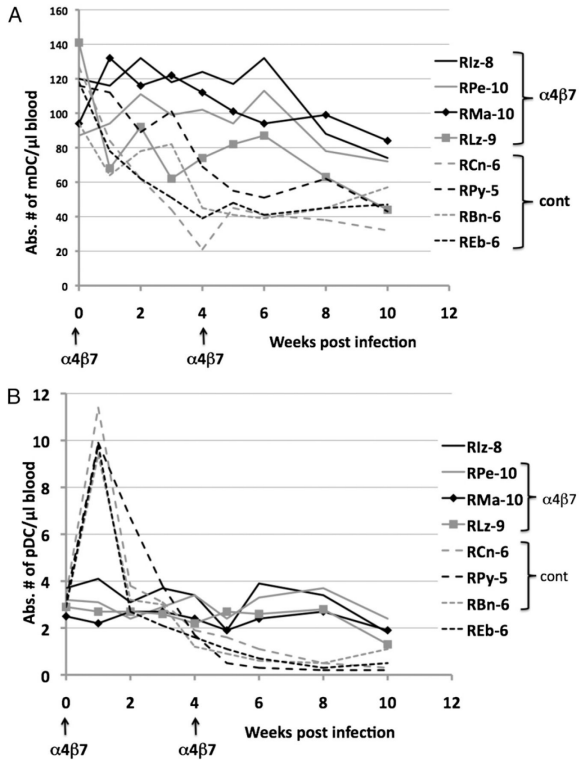

FIGURE 8.

Effect of anti-α4β7 mAb administration on the absolute numbers of (*A*) mDCs and (*B*) pDCs prior to and after SIV infection in the four anti-α4β7 mAb-treated animals (solid lines) and the four control animals (broken lines) displayed as number of cells per microliter of blood. Note the use of different scales for values of mDCs and pDCs. The levels of pDCs at week 1 in the control animals are statistically different from the α4β7-treated animals ($p = 0.021$).

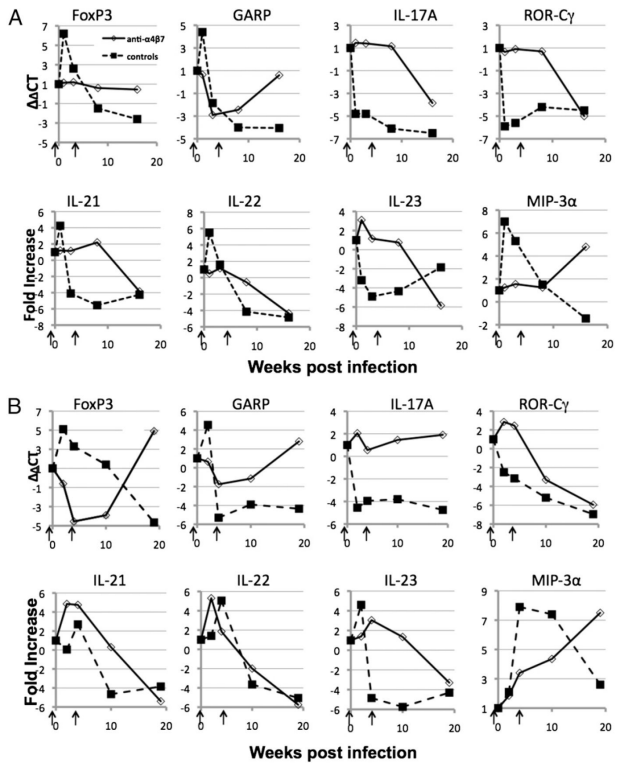

FIGURE 9.

Quantitation of relative levels of mRNA specific for FOXP3, GARP, IL-17A, ROR-Cg, IL-21, IL-22, IL-23, and MIP-3a in RNA samples isolated from (*A*) jejunal biopsies and (*B*) colorectal biopsies from the four animals treated with the anti-α4β7 mAb (solid lines) and the four control animals (broken lines). Data from the four animals in each group are reflected as median values. The values obtained in samples from the baseline studies are denoted as a value of 1. The $\Delta\Delta C_T$ values are based on values obtained on the β_2-microglobulin gene and the levels obtained on samples from baseline as per the manufacturer of the kits. The fold-increase was calculated based on values obtained on GAPDH and the values obtained on samples from the same monkey at baseline.

Table I

Summary of some of the differences in the subsets of lymphoid cells in the PBMCs of the anti-α4β7 mAb-treated animals as compared with the control animals after SIV infection

Anti-α4β7 mAb-Treated Animals	Control Animals
Biphasic increase in $CD4^+$ T cells (naive and CM)	General decrease
Initial retention and then expansion of $CCR5^+/CD4^+$ T cells	Gradual depletion of $CCR5^+/CD4^+$ T cells
Increase in $CD8^+$ T cells up to 10 wk	Increase in $CD8^+$ T cells up to 8 wk
Modest increase in $CCR5^+/CD8^+$ T cells	Marked increase in $CCR5^+/CD8^+$ T cells
Decrease in $CD25^+/CD8^+$ T cells until week 8 and then increase	Maintenance of CD25-expressing $CD8^+$ T cells
Low levels of $FOXP3^+/CD8^+$ T cells	Increase in $FOXP3^+/CD8^+$ T cells
No increase of NK cells and their subsets	Marked increases in all NK cell subsets
Gradual decrease in mDCs	More marked decrease in mDCs
Gradual decrease in pDCs	Initial marked increase and then a more marked decrease in pDCs